

We are IntechOpen, the world's leading publisher of Open Access books Built by scientists, for scientists

4,800

Open access books available

122,000

International authors and editors

135M

Downloads

Our authors are among the

154

Countries delivered to

TOP 1%

most cited scientists

12.2%

Contributors from top 500 universities

**WEB OF SCIENCE™**Selection of our books indexed in the Book Citation Index
in Web of Science™ Core Collection (BKCI)

Interested in publishing with us?
Contact book.department@intechopen.com

Numbers displayed above are based on latest data collected.

For more information visit www.intechopen.com

Design of Industrial Falling Film Evaporators

*Muhammad Wakil Shahzad, Muhammad Burhan
and Kim Choon Ng*

Abstract

The high performance evaporators are important for process industries such as food, desalination and refineries. The falling film evaporators have many advantages over flooded and vertical tubes that make them best candidate for processes industries application. The heat transfer area is the key parameter in designing of an evaporator and many correlations are available to estimate the size of tube bundle. Unfortunately, most of the correlation is available only for pure water and above 322 K saturation temperatures. Out of these conditions, the areas are designed by the extrapolation of existing correlations. We demonstrated that the actual heat transfer values are 2–3-fold higher at lower temperature and hence simple extrapolated estimation leads to inefficient and high capital cost design. We proposed an accurate heat transfer correlation for falling film evaporators that can capture both, low temperature evaporation and salt concentration effectively. It is also embedded with unique bubble-assisted evaporation parameter that can be only observed at low temperature and it enhances the heat transfer. The proposed correlation is applicable from 280 to 305 K saturation temperatures and feed water concentration ranges from 35,000 to 95,000 ppm. The uncertainty of measured data is less than 5% and RMS of regressed data is 3.5%. In this chapter, first part summarized the all available correlations and their limitations. In second part, falling film evaporation heat transfer coefficient (FFHTC) is proposed and model is developed. In the last part, experimentation is conducted and FFHTC developed and compared with conventional correlations.

Keywords: heat transfer, falling film, evaporator design, seawater evaporator

1. Introduction

The falling film evaporators currently leading in the processes industries because they have many advantages over submerged tubes evaporators. In the past, the vertical tubes evaporators were considered as most efficient but now they have been replaced by falling film evaporators due to its distinctive nature of operation. The submerged and vertical tubes evaporators are normally not fast responsive to many operational parameters. On the other hand, the falling film evaporators respond fast to feed quality and heat source supplied. These properties make them very efficient to operate across small temperature differences so that they can be arranged in cascading manners for maximum efficiency. In addition, falling film evaporators have many other advantages such as:

1.1 Advantages of falling film evaporators

The falling film evaporators have following advantages over flooded evaporators:

1. Compact design due to improved heat transfer.
2. Improved wettability provides uniform heat transfer properties across the tubes.
3. Less charge requirement, two to three times the evaporation rate.
4. Fast operation and short contact time for working fluid, favourable for food industry.
5. Falling film washed away the deposition on tubes that minimize the chances of fouling on tube surfaces.

The falling film evaporators also have many advantages over vertical tubes evaporators such as:

1. Smaller size as compared to vertical tubes for same capacity due to high heat transfer coefficient.
2. Falling film evaporator tubes are available with different corrugations to enhance the heat transfer rates as compared to vertical tube evaporators.
3. Multi pass tube bundle design for required operation as compared to single pass vertical tubes evaporators with limited operations.
4. Larger length to diameter ratio evaporator design is possible as compared to vertical tubes that help to enhance wettability and minimize the chances of dry-outs and flooding.
5. The compact design reduces the overall piping work as compared to single pass large size vertical design.
6. Due to vertical stacking arrangement, the overall footprint can be small in large industries by using falling film evaporators.

It can be seen clearly that falling film evaporators have many advantages over submerged and vertical tubes evaporators but there is lack of heat transfer data at sub-atmospheric temperature. Particularly, below 323 K, there is no data available in the literature. This was one of the main motivations for this work.

2. Heat transfer review for falling film evaporators

An efficient design of falling film evaporators is important especially for food and desalination industries. Conventionally, the empirical and theoretical correlations available in the literature are employed for the heat transfer area estimation. Most of correlations are based on different refrigerants and at near atmospheric temperature. Only few correlations are available for pure water for 322 K and above

saturation temperatures. **Table 1** provides the detail of many researchers' work related to heat transfer correlations. It also highlighted the studies of different operational parameters impact on heat transfer.

Reference	Investigators	Detail
<i>Basic correlation development</i>		
[1]	Uche et al.	Investigation of heat transfer coefficient for different heat source temperature and different flow velocities for vertical and horizontal tubes evaporators
[2]	Ribatski and Jacobi	Heat transfer coefficient values development for water and other refrigerants for horizontal evaporators fitted with single and multi tubes
[3]	Adib et al.	Experimentation on vertical tubes evaporators for heat transfer coefficient investigation. They found good agreement with published data [4–8]
[9]	Parken and Fletcher	Correlation development for non-boiling conditions
[10]	Han and Fletcher	Heat transfer coefficient correlation development for falling film evaporators for boiling conditions above 322 K saturation temperatures
[11–13]	Fujita et. al	Analytical model development for falling film evaporators with R-11 refrigerant. The measured accuracy was $\pm 20\%$
<i>Operational parameters impact investigation</i>		
[11, 14–17]	Liu et al., Fujita et al., Yang et al., Parken et al., Ribatski et al.	Film Reynold number investigation on heat transfer coefficient and main conclusions are: <ol style="list-style-type: none"> a. Heat transfer increase with Reynold number b. Heat transfer decrease to its minimum value and then increase c. Heat transfer increase to maximum and then drop
[18]	Lorenz and Yung	Investigation of single tube and multi tubes arrangement on heat transfer. They also found that the critical Reynold number is below 300 and single tube have good heat transfer as compared to array of tubes
[19]	Thome et al.	Heat transfer study on different tube geometry such as Gewa-B, plain surface, turbo-BII HP and high heat flux tubes. They found a stark difference in heat transfer values
[11]	Fujita et al.	Tubes array and feed header impact on heat transfer was studied and showed that top row has low heat transfer due to direct exposure of feed
[14]	Liu et al.	Tubes geometry impact was investigated and concluded that roll worked tubes heat transfer is 3–4 fold higher them smooth tubes
[20]	Aly et al.	Film thickness impact was studied and found that thickness has negative impact on heat transfer
[21–23]	Moeykens et al. and Chang et al	Impact of different refrigerants such as R-141b, R22, R123 and R-134a were studied and found enhanced heat transfer by additional distribution plats
[24]	Bourouni et al.	The characteristic dimensions effect was investigated and found that heat transfer enhanced significantly with increase in evaporator size

Table 1.
Literature summary on heat transfer coefficient investigation and operational parameters impact.

References	Correlation
Xu et al. [25]	$h_{\text{evaporation}} = 05.169 \times 10^{-11} \left[\frac{h_{fg} \cdot g \cdot \rho_l^2 \cdot D^2}{\Delta t^2 \cdot \mu_l} \right]^{-0.333} \left(\frac{\bar{\delta}}{D} \right)^{-0.422 \Delta t^{0.503}}$ $\cdot \left(1 + \frac{\delta_{\text{max}} - \delta_{\text{min}}}{\bar{\delta}} \right)^{5.708}$ <p>Heat source 50°C, deionized liquid, evaporator with copper tubes horizontally arranged</p>
Fujita et al. [11]	<p>First tube:</p> $\text{Nu} = \left((\text{Re}_f)^{-23} + 0.008 (\text{Re}_f)^{0.3} (\text{Pr})^{0.25} \right)^{1/2}$ <p>Second to last tubes:</p> $\text{Nu} = \left((\text{Re}_f)^{-23} + 0.01 (\text{Re}_f)^{0.3} (\text{Pr})^{0.25} \right)^{1/2}$ <p>Refrigerant Freon R-11, copper tubes with electrical heaters, diameter 25 mm</p>
Han and Fletcher [10]	$h_{\text{evaporation}} = 0.0028 \cdot \left[\frac{H_l^2}{g \cdot \rho_l^2 \cdot \mu_l^3} \right]^{-0.333} (\text{Re}_f)^{0.5} (\text{Pr})^{0.85}$ <p>Pure water, 49–127°C, electrically heated single horizontal tube, OD—50.8 mm, thickness—1.7 mm, length—254 mm</p>
Bourouni et al. [24]	$h_f = 2.2 \cdot \left[\frac{\nu_f^2}{g \cdot k_f^3} \right]^{-0.333} \cdot \left(\frac{H}{\text{OD}} \right)^{0.1} \cdot (\text{Re}_f)^{-0.333}$ <p>Pure water, 60 and 90°C, polypropylene horizontal tubes aero-evaporator, OD—25.4 mm</p>

References	Correlation
Chun and Seban [26]	$h_{\text{film}} = 0.821 \cdot \left[\frac{\mu_f^2}{g \cdot \rho_f^2 \cdot k_f^3} \right]^{-0.333} (\text{Re}_f)^{-0.22}$ Pure water, 46–118°C, vertical single tube evaporator with electrical heater, tube 28 mm diameter and 292 mm long
Alhuseini et al. [27]	Laminar regime: $h_{\text{laminar}} = 2.65 \cdot (\text{Re})^{-0.158} (\text{Ka})^{0.0563}$ Mixed regime: $h = (h^5_{\text{laminar}} + h^5_{\text{turbulent}})^{1/5}$ Pure water and Propylene glycol
Shmerler et al. [28]	$h_E = 0.0038 \cdot (\text{Re}_f)^{0.35} (\text{Pr})^{0.95}$ Vertical tube evaporator with electrical heat, water as a working fluid, tubes 25.4 mm diameter and 781 mm long
Chien et al. [29]	$\text{Nu}_{\text{cv}} = 0.0386 \cdot (\text{Re}_f)^{0.09} \cdot (\text{Re}_f)^{0.986}$ Horizontal tubes evaporator with R245fa refrigerants, operational temperature 5 and 20°C

Table 2.
 Review of heat transfer coefficient correlations for different evaporator design and operation conditions.

The heat transfer correlations available in the literature are based on different parameters and they have some limitations. **Table 2** showed most famous and widely accepted heat transfer coefficient correlations and their limitations.

The most commonly used correlation is proposed by Han and Fletcher for horizontal tube falling film evaporators. They developed this correlation for pure water at saturation temperature ranges from 322 to 393 K. It can be noticed that there are two major gaps in available literature; firstly, no data is available for evaporation heat transfer for below 322 K and secondly, there is lack of data for salt solution as boiling point elevation changes with salt concentration. These two factors are important for processes industries falling film evaporators design as most of processes are performed below 322 K such as in food and desalination industries [30–42]. This was the main motivation of this study, to provide detailed parameters for falling film evaporators design for process industries. We developed falling film heat transfer coefficient (FFHTC) correlation for saline water evaporation from 280 to 305 K saturation temperatures. We also demonstrated the effect of salt concentration on heat transfer and LMTD. This will help to design efficient falling film evaporators for processes industries.

3. Falling film heat transfer coefficient development

The idea was to modify the famous and well accepted Han and Fletcher's correlation to incorporate the different salt concentration effect and expanded to low range temperature evaporation. This will help to fill two major gaps as mentioned earlier in processes industries evaporators design.

3.1 Theoretical model

The dimensionless terms such as Nusselt, Reynolds and Prandtl numbers in the Han and Fletcher's correlation are adequate to incorporate the liquid film thermal effect in heat transfer. As per steam properties table, the specific volume of steam is rapidly changes at low temperature and it might have significant effect on heat transfer. At low temperature, the generation of microbubbles at tubes surfaces rapidly detach due to low density and it agitate the thermal barrier formed by liquid film. The conventional heat transfer correlations are not able to capture this effect. The heat transfer enhancement due to micro-bubble generation and detaching is an important phenomenon at low temperature and need to be captured in heat transfer correlation for efficient evaporator design.

The basic form of Han and Fletcher's correlation is shown in Eq. (1).

$$\frac{h_{\text{evap}} \left(\frac{\mu_l^2}{g \rho_l^2} \right)^{1/3}}{k_l} = \text{Nu} = 0.0028 (\text{Re}_l)^{0.5} (\text{Pr})^{0.85} \quad (1)$$

The constants and indices can be found from the boundary conditions of falling film evaporators. The heat supplied to the evaporator can be calculated by the energy balance of hot water circulation through the tubes as presented in Eq. (2).

$$Q_{\text{in}} = m_{\text{ch},w} C_{p,\text{ch},w} (T_{\text{ch},w}^o - T_{\text{ch},w}^i) \quad (2)$$

The overall heat transfer coefficient (U_{overall}) can be calculated by using the saturation temperatures of evaporator and log mean temperature difference (LMTD) parameters as shown in Eq. (3).

$$UA_{\text{overall}} = \frac{m_{\text{ch},w} C_{p,\text{ch},w} (T_{\text{ch},w}^{\text{out}} - T_{\text{ch},w}^{\text{in}})}{\left\{ \frac{(T_{\text{ch},w}^{\text{out}} - T_{\text{sat}}) - (T_{\text{ch},w}^{\text{in}} - T_{\text{sat}})}{\ln \left(\frac{T_{\text{ch},w}^{\text{out}} - T_{\text{sat}}}{T_{\text{ch},w}^{\text{in}} - T_{\text{sat}}} \right)} \right\}} \quad (3)$$

The Dittus-Boelter correlation can be applied to investigate the local heat transfer coefficient for falling film evaporators as shown in Eq. (4).

$$Nu = 0.023 Re^{0.25} Pr^n \quad (4)$$

Now, falling film heat transfer coefficient for evaporation can be calculated by applying Eqs. (1)–(4). The material resistance is neglected due to very thin tube wall (less than 0.7 mm). Eq. (5) presents the calculation process for falling film heat transfer coefficient.

$$\frac{1}{UA} = \left(\frac{1}{hA} \right)_{\text{tubeside}} + R_{\text{wall}} + \left(\frac{1}{hA} \right)_{\text{outside}} \quad (5)$$

The unknown parameters in Eq. (5) are calculated by the planned experiments as discussed in the following sections.

3.2 Experimental apparatus

The pilot facility of adsorption desalination (AD) cycle in Mechanical Engineering (ME) Department of NUS is utilized to investigate the unknown parameters for FFHTC correlation development. The AD pilot facility is shown in **Figure 1**.

The AD cycle has four major components such as (a) reactor beds packed with adsorbent, (b) evaporator, (c) condenser and (d) circulation pumps. In addition, there is also a conditioning facility and pre-treatment facility to perform test at an accurate conditions. The flow schematic of AD cycle is shown in **Figure 2**.

To investigate the falling film heat transfer coefficient, evaporator is designed with horizontal tubes arranged in staggered manner. There are four rows of tubes and each row has 12 tubes installed in four pass arrangements. The tubes are



Figure 1. Adsorption cycle pilot installed at NUS, Singapore (published with PI permission [43, 44]).

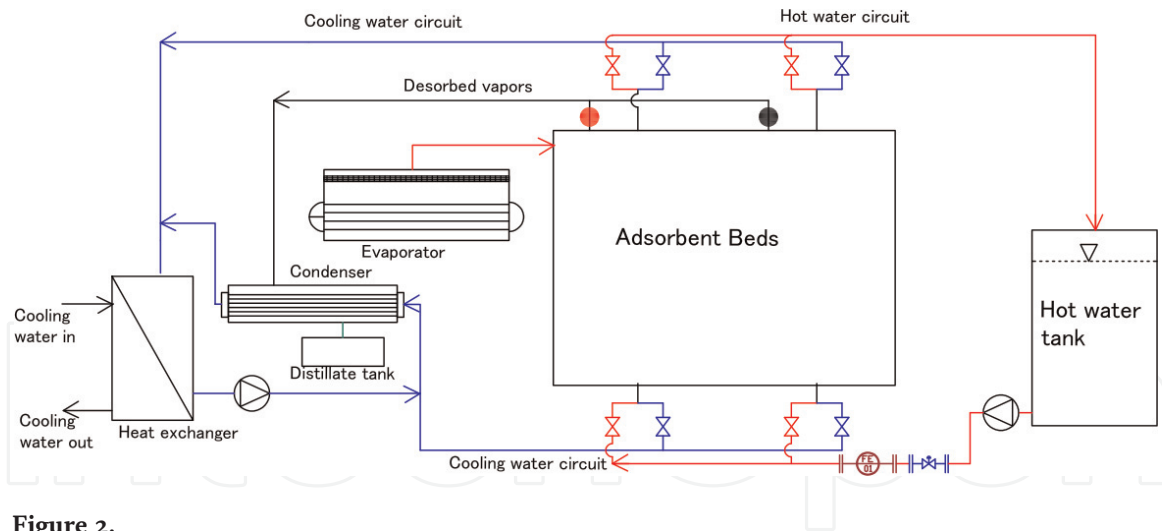


Figure 2. Adsorption cycle flow schematic with detailed components (published with author's permission [43, 44]).

Parameters	Values	Units
Number of tubes	52	
Length of each tube	2000	mm
Tube outer diameter	25	mm
Tube thickness	1.0	mm
No of passes	2	
Shell diameter	600	mm
Shell length	1800	mm

Table 3. Adsorption cycle evaporator design parameters.

fabricated with special outside and inside profile to enhance heat transfer. The design parameters of evaporator are given in **Table 3**.

3.2.1 Experimental procedure

There are three liquid circuits in the system those are important to control and maintain for a successful experiment. Firstly, the chilled water circulation through the tubes of evaporator to maintain required saturation temperature. An accurate thyristor controlled heater is installed to control chilled water temperature within ± 0.15 K. A vacuum rated feed pump help to spray water from pool of evaporator below tubes bundle to the tubes surface. To maintain the liquid level in the evaporator, the evaporated quantity refluxed back from condenser as a close loop.

Secondly, the cold water supply to the adsorption bed to remove the heat of adsorption. The adsorber bed directly communicates to evaporator to adsorb the vapors and release the heat of adsorption. This heat must be removed to maintain the vapor uptake otherwise it can be drooped to very low quantity. The cooled water flow through the cooling tower on the rooftop to reject heat to the ambient.

Lastly, the heat source to the desorber bed to regenerate the adsorbent. Once the adsorber bed fully saturated, it cannot take more vapor and it has to be regenerated for next adsorption process. The hot water is circulated through the tubes of the bed to supply heat of desorption to the adsorbent. The hot water temperature is maintained either by heater or solar thermal collectors.

Since whole system is operating at sub-atmospheric pressure so it is required to remove the non-condensable gases. A vacuum pump is connected to all the major components to remove non-condensable in case on any leakage. **Table 4** shows the operation parameters of AD cycle.

The system is instrumented with highly accurate sensors to extract real time data. For example, for pressure measurements, Yokogawa pressure transducers are installed. These sensors can measure 0–60 kPa (abs) with accuracy of $\pm 0.25\%$. Similarly, liquid flow is measured by KROHNE flow meters (accuracy $\pm 0.5\%$) and temperatures are recorded by OMEGA 10 k Ω thermistors (accuracy ± 0.15 K). All sensors are connected to Agilent system for data logging.

Parameters	Values	Units
Chilled water flow rate	50	LPM
Sea water flow rate (Γ)	1.8	LPM/m of tube length
Feed water salinity range	35,000–95,000	ppm

Table 4.
 Experimental operational parameters of adsorption pilot.

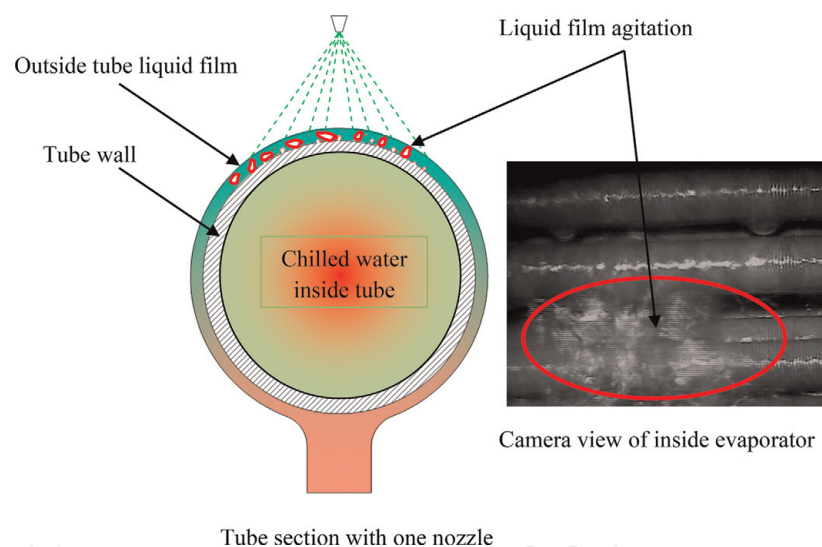


Figure 3.
 Micro-bubbles agitation of liquid film on evaporator tube surfaces captured by camera (published with author's permission [43, 44]).

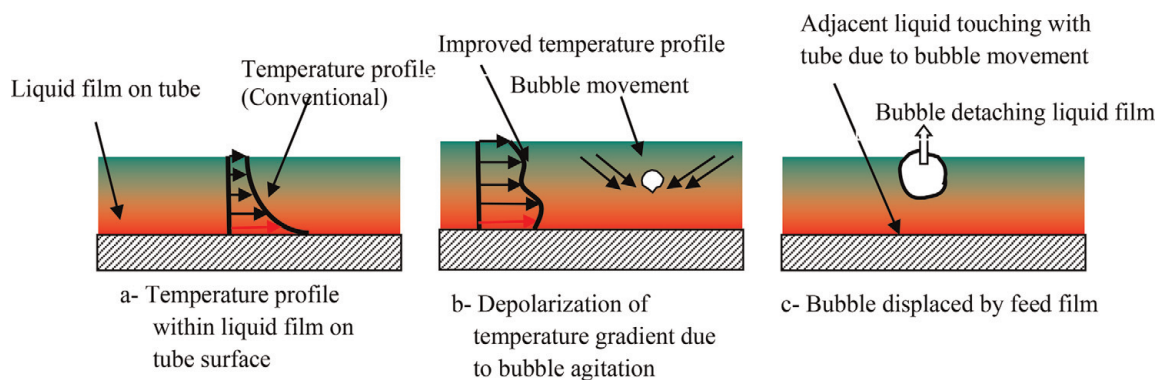


Figure 4.
 Conventional thermal barrier braking phenomenon due to bubble agitation (published with author's permission [43, 44]).

To capture the event of micro-bubble formation at low pressure, a high speed camera was installed on evaporator. The camera successfully captured the agitation of liquid film on tube surface due to formation and detaching of micro-bubbles as shown in **Figure 3**. The phenomenon of breaking the liquid thermal barrier due to film agitation is presented in **Figure 4** step by step. The natural temperature gradient within liquid film on tubes surface is the major bottle neck in heat transfer. The micro-bubble generation at low temperature agitates this barrier due to low density and produce turbulence as also captured by camera. The micro-bubble, firstly agitate the liquid film and break thermal barrier that enhance heat transfer. Secondly, when it moves up due to low density, it draw heat and provide space to adjacent liquid to have direct contact with tube surface that helps faster heat transfer rates.

4. Results and discussion

The overall heat transfer coefficient (U) was calculated at assorted heat source and salt concentrations. The evaporator chilled water temperature was varies from 10 to 40°C and salt concentration from 35,000 to 95,000 ppm. The typical trend is presented in **Figure 5** at 90,000 ppm salt concentration. The similar trend was observed at other concentration values.

The two important results can be concluded, firstly, the U values drop over 25% due to salt concentration at lower temperature but this impact is not very significant at higher temperature. This might be due to property change at higher temperature. Secondly, The U values are higher at lower temperature and this is due to micro-bubble generation and detaching phenomenon as described earlier. The same trend of U values at all concentrations strengthens the argument of micro-bubble enhanced heat transfer phenomenon.

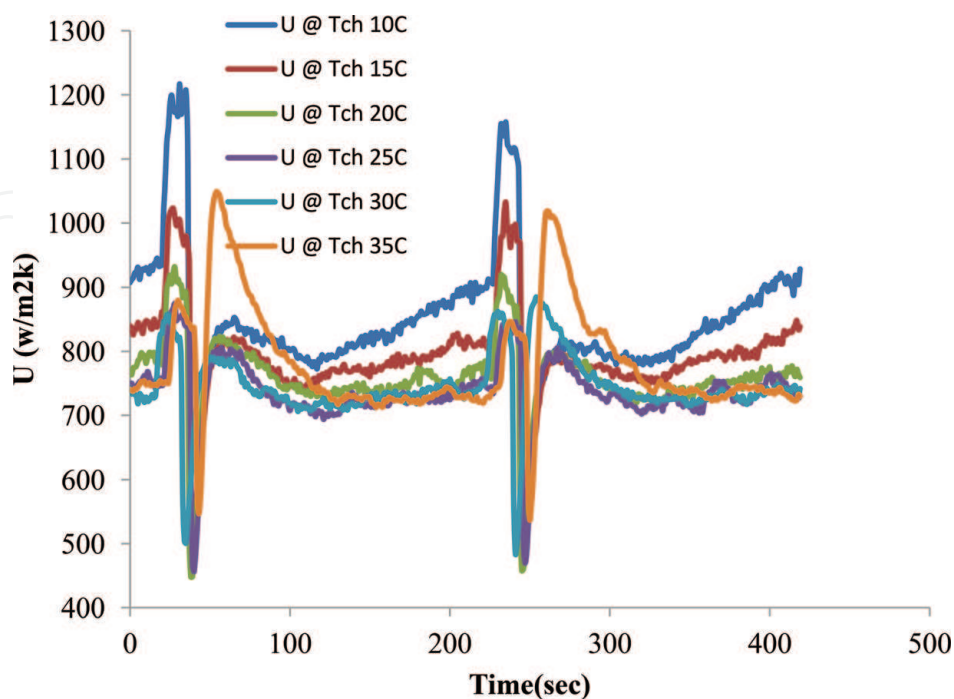


Figure 5. Overall heat transfer coefficient profiles at 90,000 ppm salt concentration and different chilled water temperatures (with author's permission [43, 44]).

The falling film heat transfer coefficient (FFHTC) values are then calculated by using the methodology presented in the earlier section and presented in **Figure 6**. It can be noticed that FFHTC follows the same trend as U values at assorted heat source and salt concentrations.

The noticeable point in the plot is the heat transfer coefficient values drop initially with drop in evaporator vapor space temperature and achieve minimum values at 300 K. Once the vapor space temperature dropped further down, the heat transfer values start increasing. The increasing trend is even sharper below 295 K vapor space temperature and this is because of rapid change in vapor specific volume. The vapor specific volume change can divide the evaporation processes into three categories; namely, film surface evaporation, transition and micro-bubble assisted evaporation. The sharp change in specific volume below 295 K help to generate micro-bubble that detach from tube surface immediately due to low density and agitate the thermal barrier resulting increase in heat transfer rates. This phenomenon is observed and captured for the first time and named as “micro-bubble assisted film evaporation”.

It can be clearly noticed that micro-bubbles play an important role at low temperature to enhance the heat transfer. The traditional heat transfer coefficient correlations are not able to capture this unique phenomenon. All correlations available in the literature can only work in film surface evaporation zone. Their extrapolation to capture transition and micro-bubble assisted zone also cannot predict an accurate value and heat exchanger designed based on these values cannot perform up to the level. Hence there is an urgent need for the development of an accurate heat transfer coefficient correlation to capture these two zones for efficient heat exchanger design.

A new correlation is proposed for falling film heat transfer coefficient that can efficiently capture transition and micro-bubble assisted evaporation at assorted salt concentration. The proposed model was written in FORTRAN and fitted with experimental data conditions. All important parameters such as heat flux, flow velocity and vapor properties were also included. Most importantly, the salt concentration and vapor specific volume parameters those were missing in conventional correlations are also embedded in the proposed correlation as shown in Eq. (6) [48, 49].

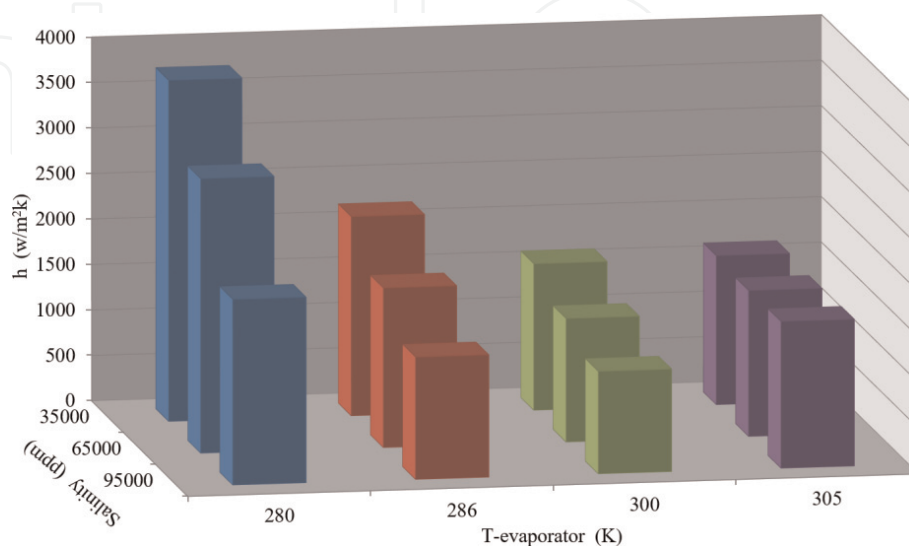


Figure 6. Experimental film evaporation heat transfer coefficient profiles at different saturation temperature and different salt concentrations (with author's permission [43, 44]).

$$h_{fallingfilm} = \left\{ 0.279 \left(\frac{\mu_l^2}{g \cdot \rho_l^2 K_l^3} \right)^{-0.333} (Re_\Gamma)^{-2.18} (Pr)^{4.0} \left(2 \cdot \exp \left(\frac{S}{30000} \right) - 1 \right)^{-0.45} \cdot \left(\frac{T_{evap}}{322} \right) \right\} + \left\{ 0.875 \left(\frac{q}{DT} \right) \cdot \left(\frac{V_{evap}}{52.65} \right) \right\} \quad (6)$$

The proposed correlation is applicable from 280 to 305 K saturation temperatures. It also captures the feed water concentration ranges from 35,000 to 95,000 ppm. The film Reynolds number (Re_Γ) ranges from 45 to 90 and Prandtl number (Pr) from 5 to 10. In proposed correlation, the first term control the thermally driven evaporation and second terms capture bubble assisted evaporation phenomenon that is missing in the conventional correlations. The proposed model results are presented in **Figure 7**. It can be noticed that model has good agreement with experimental results. The uncertainty of measured data is less than 5% and RMS of regressed data is 3.5%.

Conventionally, the Han and Fletcher correlation is applied in the industry for low temperature ranges with its extrapolated results. The comparison of actual heat transfer values calculated by the experiments is compared with extrapolated Han and Fletcher values and it can be observed from **Figure 8** that there is huge difference. The conventional Han and Fletcher correlation can only capture film evaporation zone accurately but bubble assisted evaporation is totally out of range. The unique feature of “bubble assisted evaporation” can only be captured by the proposed falling film heat transfer coefficient correlation that boost heat transfer 2–3 fold. As a result, for process industries where the saturation temperature is below 295 K, the evaporator can be compact and low cost as compared to current design. The proposed correlation is timely and important for efficient design of falling film evaporator for process industries.

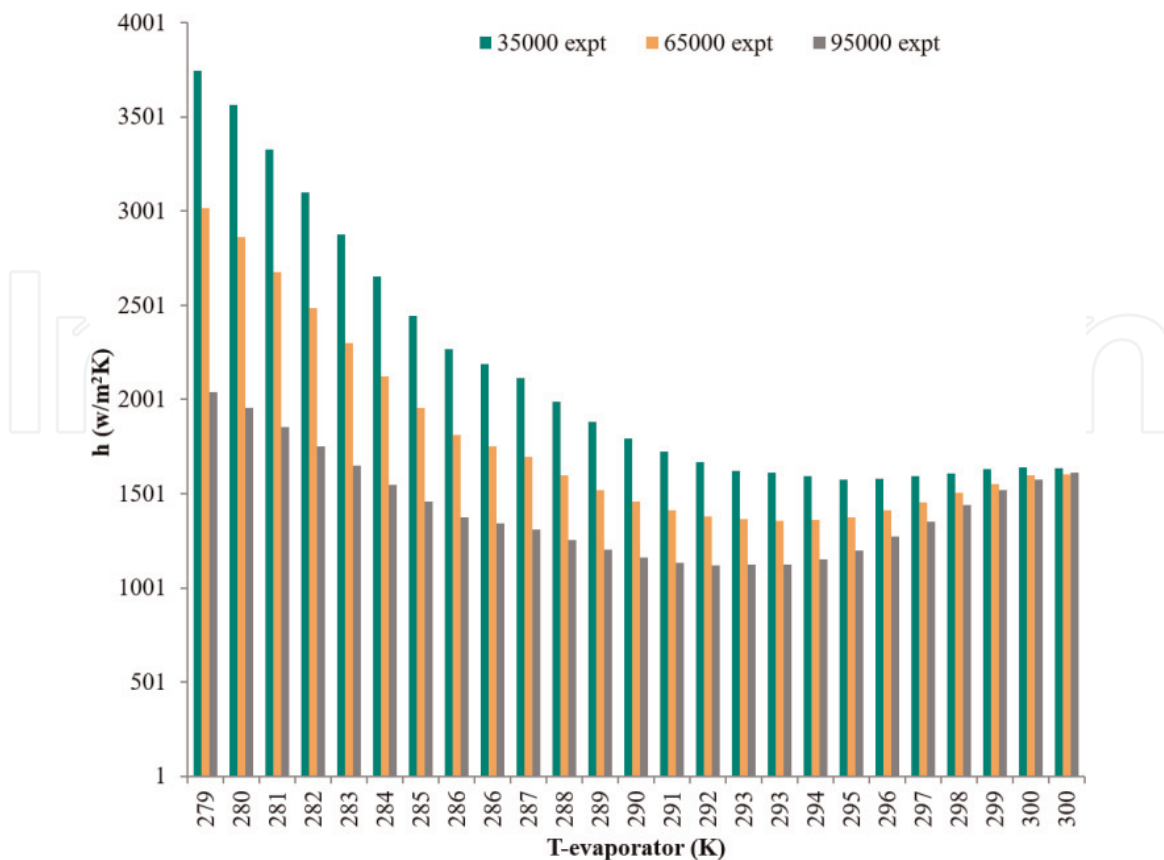


Figure 7.

The proposed falling film heat transfer coefficient correlation with experimental results (with author's permission [43, 44]).

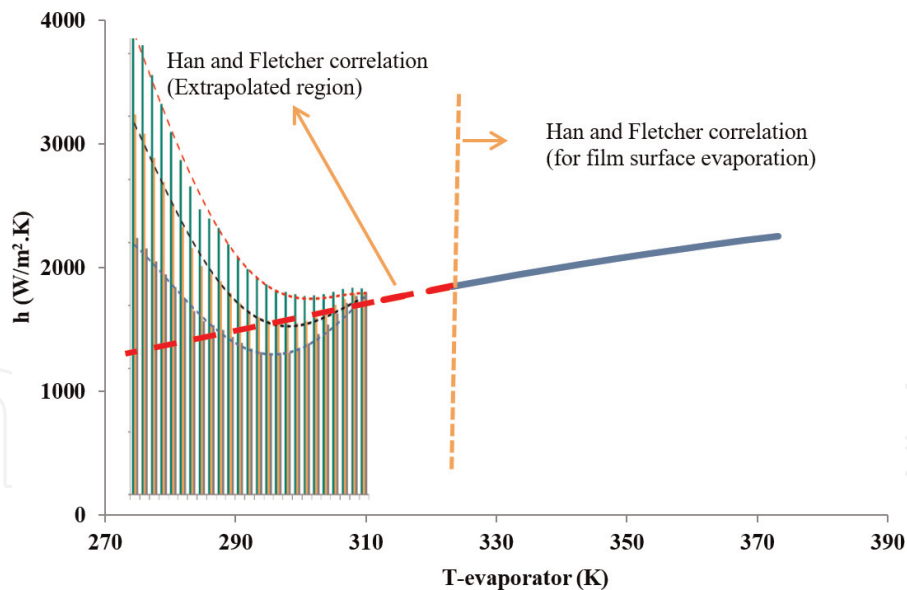


Figure 8.
 Proposed falling film heat transfer coefficient compared with conventional Han & Fletcher's extrapolated values (with author's permission [43, 44]).

5. Summary

The horizontal falling film evaporators have many advantages over submerged and vertical tubes evaporators. Currently, there is no heat transfer correlation that can capture evaporation at low temperature especially below 295 K with different salt concentration. This is very important for efficient design of process evaporators. A horizontal tube falling film heat transfer coefficient correlation is proposed to capture effect, low temperature and salt concentration. It is demonstrated that the actual heat transfer values at low temperature can be 2–3 fold higher than the estimated values due to unique bubble-assisted evaporation phenomenon. The proposed correlation is applicable from 280 to 305 K saturation temperatures and feed water concentration ranges from 35,000 to 95,000 ppm. The uncertainty of measured data is less than 5% and RMS of regressed data is 3.5%.

Acknowledgements

Authors would like to thanks to KAUT and NUS for this study. The data is reproduced by the author's permission [44].

Nomenclature

μ_l	liquid viscosity (kg/m-s)
k_l	liquid conductivity (W/m K)
Pr	Prandtl number
q	input heat flux (W/m ²)
T_{evap}	evaporator saturation temperature (K)
$T_{\text{saturation}}$	evaporator saturation temperature (K)
$T_{\text{ch, in}}$	chilled water inlet temperature (K)
v_g	vapor specific volume (m ³ /kg)
ΔT	$T_{\text{ch, out}} - T_{\text{evap}}$

ρ_l	liquid density (kg/m ³)
Re_f	Film Reynolds number
S	feed water salinity (ppm)

Abbreviations

EHTC	evaporation heat transfer coefficient
FFEHTC	falling film evaporation heat transfer coefficient
MED	multi-effect desalination
MSF	multi stage flash evaporation
AD	adsorption desalination
LMTD	log mean temperature difference
ppm	part per million

IntechOpen

Author details

Muhammad Wakil Shahzad*, Muhammad Burhan and Kim Choon Ng
Water Desalination and Reuse Center (WDRC), King Abdullah University of
Science and Technology, Thuwal, Saudi Arabia

*Address all correspondence to: mohammad.shahzad@kaust.edu.sa

IntechOpen

© 2019 The Author(s). Licensee IntechOpen. This chapter is distributed under the terms of the Creative Commons Attribution License (<http://creativecommons.org/licenses/by/3.0>), which permits unrestricted use, distribution, and reproduction in any medium, provided the original work is properly cited. 

References

- [1] Uche J, Artal J, Serra L. Comparison of heat transfer coefficient correlations for thermal desalination units. *Desalination*. 2002;**152**:195-200
- [2] Ribatski G, Jacobi AM. Falling film evaporation on horizontal tubes—A critical review. *International Journal of Refrigeration*. 2005;**28**:635-653
- [3] Adib TA, Heyd B, Vasseur J. Experimental results and modeling of boiling heat transfer coefficients in falling film evaporator usable for evaporator design. *Chemical Engineering and Processing*. 2009;**48**: 961-968
- [4] Chun KR, Seban RA. Heat transfer to evaporating liquid films. *Transactions of the the American Society of mechanical Engineers: Journal of Heat Transfer*. 1971;**93**(C):391-396
- [5] Prost JS, Gonzaalez MT, Urbicain MJ. Determination and correlation of heat transfer coefficients in a falling film evaporator. *Journal of Food Engineering*. 2006;**4**(73):320-326
- [6] Ahmed SY, Kaparathi R. Heat transfer studies of falling film heat exchangers. *Indian Journal of Technology*. 1963;**1**: 377-381
- [7] McAdams WH, Drew TB, Bays GS. Heat transfer to falling—Water films. *Transactions of American Society of mechanical Engineers*. 1940;**62**:627
- [8] Herbert LS, Stern UJ. An experimental investigation of heat transfer to water in film flow. *Canadian Journal of Chemical Engineering*. 1968; **46**:401-407
- [9] Parken WH, Fletcher LS. An experimental and analytical investigation of heat transfer to thin water films on horizontal tubes. Report UVA-526078-MAE. University of Virginia; 1977. pp. 77-101
- [10] Han JC, Fletcher LS. Falling film evaporation and boiling in circumferential and axial grooves on horizontal tubes. *Industrial and Engineering Chemistry Process Design and Development*. 1985;**24**:570-575
- [11] Fujita Y, Tsutsui M. Experimental investigation of falling film evaporation on horizontal tubes. *Heat Transfer-Japanese Research*. 1998;**27**:609-618
- [12] Fujita Y, Tsutsui M, Zhou Z-Z. Evaporation heat transfer of falling films on horizontal tube—Part 1, analytical study. *Heat Transfer-Japanese Research*. 1995;**24**:1-16
- [13] Fujita Y, Tsutsui M, Zhou Z-Z. Evaporation heat transfer of falling films on horizontal tube—Part 2, experimental study. *Heat Transfer-Japanese Research*. 1995;**24**:17-31
- [14] Liu ZH, Yi J. Falling film evaporation heat transfer of water/salt mixtures from roll-worked enhanced tubes and tube bundle. *Applied Thermal Engineering*. 2002;**22**(1):83-95
- [15] Yang LP, Shen SQ. Experimental study of falling film evaporation heat transfer outside horizontal tubes. In: *Conference on Desalination and the Environment*; Halkidiki, Greece. 2007
- [16] Parken WH et al. Heat-transfer through falling film evaporation and boiling on horizontal tubes. *Journal of Heat Transfer—Transfer The American Society of mechanical Engineers*. 1990; **112**(3):744-750
- [17] Ribatski G, Thome JR. Experimental study on the onset of local dryout in an evaporating falling film on horizontal plain tubes. *Experimental Thermal and Fluid Science*. 2007;**31**(6):483-493

- [18] Lorenz JJ, Yung D. Film breakdown and bundle-depth effects in horizontal tube, falling-film evaporators. *Journal of Heat Transfer—Transfer The American Society of mechanical Engineers*. 1982; **104**(3):569-571
- [19] Roques JF, Thome JR. Falling films on arrays of horizontal tubes with R-134a. Part II: Flow visualization, onset of dry out, and heat transfer predictions. *Heat Transfer Engineering*. 2007; **28**(5): 415-434
- [20] Aly G, Al-Hadda A, Abdel-Jawad M. Parametric study on falling film seawater desalination. *Desalination*. 1997; **65**:43-55
- [21] Moeykens S, Pate MB. Spray evaporation heat transfer performance of R-134a on plain tubes. *ASHRAE Transactions*. 1994; **100**(2):173-184
- [22] Moeykens S, Kelly JE, Pate MB. Spray evaporation heat transfer performance of R-123 in tube bundles. *ASHRAE Transactions*. 1996; **102**(2): 259-272
- [23] Chang TB, Chiou JS. Spray evaporation heat transfer of R-141b on a horizontal tube bundle. *International Journal of Heat and Mass Transfer*. 1998; **42**:1467-1478
- [24] Bourouni K, Martin R, Tadriss L, Tadriss H. Modelling of heat and mass transfer in a horizontal tube falling film evaporators for water desalination. *Desalination*. 1998; **116**:165-184
- [25] Xu L, Ge M, Wang S, Wang Y. Heat transfer film coefficients of falling film horizontal tube evaporators. *Desalination*. 2004; **166**:223-230
- [26] Chun KR, Seban RA. Heat transfer to evaporating liquid films. *The American Society of mechanical Engineers Journal of heat transfer*. 1971; **11**:391-396
- [27] Alhousseini AA, Tuzla K, Chen JC. Falling film evaporation of single component liquids. *International Journal of Heat and Mass Transfer*. 1998; **41**(12):1623-1632
- [28] Shmerler JA, Mudawwar I. Local evaporative heat transfer coefficient in turbulent free-falling liquid films. *International Journal of Heat and Mass Transfer*. 1988; **31**(4):731-742
- [29] Chien LH, Tsai YL. An experimental study of pool boiling and falling film evaporation on horizontal tubes in R-245fa. *Applied Thermal Engineering*. 2011; **31**:4044-4054
- [30] Shahzad MW, Burhan M, Ng KC. The fallacy of energy efficiency for comparing desalination plants: A standard primary energy approach. *Nature Clean Water*. DOI: 10.1038/s41545-018-0028-4
- [31] Shahzad MW, Burhan M, Ghaffour N, Ng KC. A multi evaporator desalination system operated with thermocline energy for future sustainability. *Desalination*. 2018; **435**: 268-277
- [32] Shahzad MW, Burhan M, Son HS, Seung Jin O, Ng KC. Desalination processes evaluation at common platform: A universal performance ratio (UPR) method. *Applied Thermal Engineering*. 2018; **134**:62-67
- [33] Ng KC, Shahzad MW. Sustainable desalination using ocean thermocline energy. *Renewable and Sustainable Energy Reviews*. 2018; **82**:240-246
- [34] Shahzad MW, Burhan M, Ng KC. Pushing desalination recovery to the maximum limit: Membrane and thermal processes integration. *Desalination*. 2017; **416**:54-64. DOI: 10.1016/j.desal.2017.04.024
- [35] Ng KC, Shahzad MW, Son HS, Hamed OA. An exergy approach to

efficiency evaluation of desalination. *Applied Physics Letters*. 2017;**110**: 184101. DOI: 10.1063/1.4982628

[36] Shahzad MW, Burhan M, Li A, Ng KC. Energy-water-environment nexus underpinning future desalination sustainability. *Desalination*. 2017;**413**:52-64

[37] Shahzad MW, Ng KC. An improved multi-evaporator adsorption desalination cycle for GCC countries. *Energy Technology*. 2017. DOI: 10.1002/ente.201700061

[38] Shahzad MW, Ng KC, Thu K. Future sustainable desalination using waste heat: Kudos to thermodynamic synergy. *Environmental Science: Water Research & Technology*. 2016;**2**:206-212

[39] Thu K, Kim Y-D, Shahzad MW, Saththasivam J, Ng KC. Performance investigation of an advanced multi-effect adsorption desalination (MEAD) cycle. *Applied Energy*. 2015;**159**:469-477

[40] Shahzad MW, Thu K, Kim Y-d, Ng KC. An experimental investigation on MEDAD hybrid desalination cycle. *Applied Energy*. 2015;**148**:273-281

[41] Ng KC, Thu K, Seung Jin O, Li A, Shahzad MW, Ismail AB. Recent developments in thermally-driven seawater desalination: Energy efficiency improvement by hybridization of the MED and AD cycles. *Desalination*. 2015; **356**:255-270

[42] Shahzad MW, Ng KC, Thu K, Saha BB, Chun WG. Multi effect desalination and adsorption desalination (MEDAD): A hybrid desalination method. *Applied Thermal Engineering*. 2014;**72**:289-297

[43] Shahzad MW, Myat A, Gee CW, Ng KC. Bubble-assisted film evaporation correlation for saline water at sub-atmospheric pressures in horizontal-tube evaporator. *Applied Thermal Engineering*. 2013;**50**:670-676

[44] Shahzad MW. The hybrid multi-effect desalination (MED) and the adsorption (AD) cycle for desalination [doctoral thesis]. National University of Singapore; 2013